The Topology of Lysine-Containing Amphipathic Peptides in Bilayers by Circular Dichroism, Solid-State NMR, and Molecular Modeling

Bas Vogt,* Philippe Ducarme,† Susan Schinzel,* Robert Brasseur,† and Burkhard Bechinger*
*Max-Planck-Institut für Biochemie, 82152 Martinsried, Germany; and †Centre de Biophysique Moléculaire Numérique, Faculté Universitaire des Sciences Agronomique de Gembloux, Passage des Déportés, 5030 Gembloux, Belgium

ABSTRACT In order to better understand the driving forces that determine the alignment of amphipathic helical polypeptides with respect to the surface of phospholipid bilayers, lysine-containing peptide sequences were designed, prepared by solid-phase chemical synthesis, and reconstituted into membranes. CD spectroscopy indicates that all peptides exhibit a high degree of helicity in the presence of SDS micelles or POPC small unilamellar vesicles. Proton-decoupled ^{31}P-NMR solid-state NMR spectroscopy demonstrates that in the presence of peptides liquid crystalline phosphatidylcholine membranes orient well along glass surfaces. The orientational distribution and dynamics of peptides labeled with ^{15}N at selected sites were investigated by proton-decoupled ^{15}N solid-state NMR spectroscopy. Polypeptides with a single lysine residue adopt a transmembrane orientation, thereby locating this polar amino acid within the core region of the bilayer. In contrast, peptides with $\geq$3 lysines reside along the surface of the membrane. With 2 lysines in the center of an otherwise hydrophobic amino acid sequence the peptides assume a broad orientational distribution. The energy of lysine discharge, hydrophobic, polar, and all other interactions are estimated to quantitatively describe the polypeptide topologies observed. Furthermore, a molecular modeling algorithm based on the hydrophobicities of atoms in a continuous hydrophilic-hydrophobic-hydrophilic potential describes the experimentally observed peptide topologies well.

INTRODUCTION

Whereas helical secondary structure elements are important building blocks of membrane proteins (Deisenhofer et al., 1985; Picot et al., 1994; Doak et al., 1996; Belrhali et al., 1999), they also interact with phospholipid membranes as independent units, where they assume transmembrane or in-plane configurations (Dempsey, 1990; Segrest et al., 1990; Sansom, 1993). Amphipathic helical peptides of $\geq$12 residues have been shown to exhibit strong antimicrobial activity, in many cases without affecting the survival rate of vertebrate cells at similar concentrations (Hoffmann et al., 1983; Gibson et al., 1986; Hultmark, 1994; Vogt and Bechinger, 1999). Many species store these peptides for immediate release, thereby providing systems of fast response against bacterial, fungal, or viral infections (Bevins and Zasloff, 1990; Boman, 1995; Bechinger, 1999). These defense systems include cecropins in insects, magainins in amphibians, or defensins in humans. Even more interesting for potential pharmaceutical applications is the finding that some of these peptides selectively lyse certain tumors over healthy vertebrate cells (Cruciani et al., 1991; Ohsaki et al., 1992; Haimovich and Tanaka, 1995; Soballe et al., 1995).

Magainins and cecropins constitute large families of polypeptides composed of 20–40 amino acids (reviewed in Bechinger, 1999). No primary sequence homology is obvious within or between the families; the peptides are, however, highly water-soluble due to the abundance of lysine residues within their sequence. Magainin antibiotic peptides have been shown to decouple the ionic gradient across bacterial or spermatozoal cells, isolated mitochondria, or reconstituted cytochrome oxidase liposomes, thereby depriving the organisms of their major source of energy (Juretic et al., 1994; Bechinger, 1999 and references cited therein). In electrophysiological recordings these peptides have also been shown to interact with planar lipid membranes, thereby causing bilayer disruption or, in some experiments, channel-like activities (Duclohier et al., 1989; Cruciani et al., 1992). CD-, FTIR-, Raman-, and NMR-spectroscopies indicate that magainins and cecropins adopt amphipathic α-helix conformations in membrane-like environments (Bechinger, 1999 and references cited therein).

Several models have been suggested to explain the antibiotic and the pore-forming activities of lysine-containing amphipathic peptides (Bechinger, 1999). These include the formation of transmembrane helical bundles in which the hydrophilic residues are directed into the central water-filled pore, whereas at the same time apolar residues interact with the hydrophobic core region of the membrane (Vaz Gomes et al., 1993). The accumulation of positively charged residues in the ion-conducting cavity of these bundles suggests the formation of a pore that favors the passage of anions. In contrast, cation selectivity is observed for these openings in the presence of negatively charged phospholip-

Received for publication 20 May 1999 and in final form 9 August 2000.

Address reprint requests to Burkhard Bechinger, Max-Planck-Institut für Biochemie, Am Klopferspitz 18a, 82152 Martinsried, Germany. Tel.: +49-89-8578-2466; Fax: +49-89-8578-2876; E-mail: bechinge@biochem.mpg.de.

Abbreviations used: CD, circular dichroism; FTIR, Fourier transform infrared spectroscopy; E_{int}, transfer energy of molecules taking accessible atomic area into account; E_{lip}, energy of lipid bilayer perturbation; E_{tr}, atomic transfer energy; Fmoc, 9-fluorenylmethyloxycarbonyl; H, transfer energy of molecules; HPLC, high-performance liquid chromatography; NMR, nuclear magnetic resonance; POPC, 1-palmitoyl-2-oleoyl-*sn*-glycero-3-phosphocholine; SDS, sodium dodecyl sulfate; TFE, trifluoroethanol.

0006-3495/00/11/2644/13 $2.00

ids (Cruciani et al., 1992). A modification of this model, therefore, incorporates a high density of acidic phospholipids, which in conjunction with basic peptides coat the lumen of the "wormholes" formed (Cruciani et al., 1992; Ludtke et al., 1996). The interactions that allow for the stable formation of such aggregates in the membranes have so far not been quantified.

However, solid-state NMR structural data indicate the magainin α-helix axis is oriented approximately parallel to the membrane surface (Bechinger et al., 1993). These data have been confirmed by fluorescence energy transfer measurements in which tryptophan replacements at positions 5, 12, and 16 of magainin 2 have all been shown to be located $\sim$10 Å from the bilayer center (Matsuzaki et al., 1994). In such a configuration, lysines and other polar and charged residues are well-separated from the hydrophobic bilayer interior. These structural data indicate that the detergent-like properties of amphipathic polypeptides should also be considered as the reason for their antibiotic activity (Bechinger, 1999).

The rarely occurring step-wise increases in bilayer conductivity that have been observed in some electrophysiological recordings are, however, more difficult to explain by peptides resting in in-plane orientations. The structural findings by NMR and fluorescence spectroscopies (Bechinger et al., 1993; Matsuzaki et al., 1994), the comparison with the "pore-forming activity" of detergents (cf. literature cited in Bechinger, 1997, 1999), and the large fluctuations of the step size in electrophysiological recordings over several orders of magnitude (Duclohier et al., 1989; Cruciani et al., 1992; Haimovich and Tanaka, 1995) have channeled in the suggestion that stochastic fluctuations in the local peptide surface density result in the transient destabilization of the bilayer packing concomitant with increased ion conductivity (Bechinger, 1997).

The structure determination by physical techniques forms a valuable starting point to analyze the conformational space and the dynamics of biomolecules. The techniques that provide high-resolution structures of biomolecules, such as diffraction techniques or NMR spectroscopy, however, sample on homogenous ensembles of low-energy conformations. In contrast, single-channel electrophysiological recordings are designed to focus on single or a few events at a time, which are not necessarily caused by molecules in their lowest energetic state. It is, therefore, possible that the formation of transmembrane aggregates by amphipathic helical peptides is a rare event, which is not observed by high-resolution structural techniques (Bechinger, 1997, 1999). Only a detailed knowledge of the energies involved in the reorientation and assembly of these molecules can provide insight into the probabilities of transmembrane bundle formation and, therefore, allows one to evaluate the models presented.

Previously, a formalism was presented to quantitatively analyze the pH-dependent equilibria of histidine-containing peptides that are either oriented along the bilayer surface or occur in a transmembrane configuration (Bechinger, 1996; Bechinger et al., 1999a, b). The peptides presented in this paper were designed and prepared by solid-phase peptide synthesis in order to test for the influence of lysine residues on the orientation of helical polypeptides with respect to the membrane normal. The lysines were placed along the sequence in such a manner that amphipathic α-helices with increasing numbers of lysines form. In addition, by positioning the residues at different locations the possibility of lysine side chain snorkeling was investigated. The helical secondary structure of these peptides is confirmed by CD spectroscopy, thereafter the alignment of the helix axis with respect to the normal of oriented lipid bilayers is determined by proton-decoupled ^{15}N solid-state NMR spectroscopy (Bechinger et al., 1999a). Due to the abundance and the relative importance of lysines in some families of amphipathic peptide antibiotics, the role of this amino acid for the alignment of some designed peptide helices is investigated. Hydrophobic and polar interactions and the number and placement of lysine residues in these sequences are taken into account during a theoretical analysis. The experimental data will also be compared using a molecular modeling algorithm designed independently to predict the orientation and the penetration of peptides with respect to the surface of membrane mimetic environments (Ducarme et al., 1998). As others did (Ben-Shaul et al., 1996; Ben-Tal et al., 1996; La Rocca et al., 1999) this algorithm describes the membrane as a continuous medium with constant properties within planes parallel to the membrane surface and characteristics varying with the membrane depth.

MATERIALS AND METHODS

Peptide synthesis

The peptides were prepared by solid-phase peptide synthesis on ABI 431 or Millipore 9030 automated peptide synthesizers, respectively, using Fmoc chemistry. The sequences and their abbreviations used in the text are the following:

KKLAL ALALA LKALA LALAL KKA	LAK_1
KKLLL LLKLL LLLLL KLLLL KK	$LK_2^{<260}$
KKLLK LLLLL LLLLL KLLLL KK	$LK_2^{<320}$
KKLKL LLLLL LLKLL LLLLL KK	$LK_2^{<160}$
KKLAL ALAKA LAKAL KLALA LAKK	LAK_3
KKLAK ALAKA LAKAL KLALA LAKK	LAK_4

The superscripts <260 and <320 refer to the hydrophobic angle, which is the widest angle separating the lysines in bold in an Edmundson's helical wheel diagram (see Fig. 2). At the doubly underlined positions ^{15}N-labeled Fmoc-protected amino acid analogs (Promochem, Wesel, Germany) were incorporated. The lysine residues in the central portion of the peptide that are the focus of this investigation are shown in bold; the terminal lysine residues are added to increase the peptide solubility and to anchor the peptide with respect to the membrane interface. The identity and purity of the peptides were analyzed by reversed-phase HPLC and matrix-assisted laser desorption ionization mass spectrometry (MALDI-MS).

CD spectroscopy

Circular dichroism spectra were recorded on an auto-dichrograph mark IV (Jibon-Yvon) in the range 190–250 nm using quartz cuvettes with a 0.2 mm pathlength. Ten scans were averaged and corrected for contributions of SDS micelles or POPC small unilamellar vesicles and buffer (20 mM Tris/H_2SO_4, pH 7.2). The peptide-SDS ratios were 1/300 (mol/mol) at a peptide concentration of 100 μM. The molar ellipticity was calculated using *d*-10-camphorsulfonic acid ($\Theta_{290,5}$ = 7783° cm^2 dmol^{-1}) as a reference (Chen and Yang, 1977). The line shapes of the spectra were analyzed using a least-square fitting routine by comparison to polylysine standards representing 100% α-helix, β-turn, or random coil, respectively.

Solid-state NMR spectroscopy

Oriented samples for solid-state NMR spectroscopy were prepared by dissolving 15 mg of peptide in TFE/water mixtures. The pH of the sample was adjusted to neutral by addition of the appropriate amounts of 1 N NaOH. Typically, 200 mg POPC (Avanti Polar Lipids, Birmingham, AL) was added to the sample. The homogenous mixture was applied onto 30–35 thin coverglasses (11 × 22 mm), dried, and exposed to high vacuum over night. After the samples had been equilibrated in an atmosphere of 93% relative humidity the glass plates were stacked on top of each other and sealed. The membrane stacks were introduced into the flat coil of a home-built solid-state NMR probe head (Bechinger and Opella, 1991) with the normal of the glass plates (lipid bilayers) oriented parallel to the magnetic field direction. Proton-decoupled ^{15}N solid-state NMR spectra were acquired on a wide-bore Bruker AMX400 spectrometer using a cross-polarization pulse sequence (Pines et al., 1973). The sample was cooled during data acquisition with a stream of air at ambient temperature. Typical acquisition parameters were: spin lock time 1.6 ms, recycle delay 3 s, ^{1}H B_1-field 1 mT, 254 data points, and spectral width 40 kHz. An exponential apodization function (corresponding to a line-broadening of 300 Hz) was applied before Fourier transformation. Chemical shift values are referenced with respect to $(NH_4)_2SO_4$ (27 ppm).

Proton-decoupled ^{31}P solid-state NMR spectra were recorded to analyze the orientational distribution of the phospholipids using a Hahn-echo pulse sequence with proton decoupling (Rance and Byrd, 1983). The ^{31}P 90° pulses ranged from 3.5 to 5.5 μs and the recycle delay was 2 s.

Molecular modeling calculations

The assumption is made that properties of the membrane are constant in the plane of the bilayer (*x* and *y* axes). Thus, the lipid/water interfaces are described by a function, $C_{(z)}$, which varies along the *z* axis only; *z* (in Ångstroms) is perpendicular to the plane of the membrane and its origin is at the center of the bilayer. $C_{(z)}$ is an empirical function varying from 0.5 (completely hydrophilic) to −0.5 (completely hydrophobic). It is derived from Milik and Skolnick (1993):

$$C_{(z)} = 0.5 - \frac{1}{1 + e^{\alpha(|z| - z_0)}} \quad (1)$$

where α and z_0 are mathematical parameters calculated with $C_{(z=13.5\text{Å})} = -0.49$ and $C_{(z=18\text{Å})} = 0.49$, and that this symmetrical function is approximately constant from $-\infty$ to −18 Å (hydrophilic phase), −13.5 Å to 13.5 Å (hydrocarbon core), and 18 Å to ∞ (hydrophilic phase). Z = 13.5 Å is the distance at which the first polar heads appear (White, 1994), and an interface of 4.5 Å gives the best results for the simulation. The same interface width was found in the Monte Carlo technique developed by Milik and Skolnick (1993). This mathematical form of $C_{(z)}$ was chosen because it is continuous and can be rapidly computed.

To calculate the restraints we use atomic surface transfer energies. This concept relies on the assumption that the overall transfer energy of a molecule, *H*, can be calculated as

$$H = \sum_{i=1}^{N} S_{(i)} E_{tr(i)} \quad (2)$$

where *i* is an index for the N atoms of the molecule, *S* (Å^2) is the solvent-accessible surface (calculated by using the NSC routine (Eisenhaber and Argos, 1993)), and E_{tr} (kJ/mol Å^2) is the transfer energy by surface of individual atoms (Ducarme et al., 1998).

To build restraints, one must define the general structural features of integral membrane proteins. The segregation of hydrophobic and hydrophilic parts of the molecule imposed by the interface is due to the hydrophobic effect. To simulate this, for each configuration of the system, we calculate the interface restraint as

$$E_{int} = -\sum_{i=1}^{N} S_{(i)} E_{tr(i)} C_{(zi)} \quad (3)$$

The general behavior of Eq. 3 is that E_{int} increases when solvent-accessible hydrophilic atoms (i.e., $E_{tr} > 0$) penetrate the membrane and decreases when solvent-accessible hydrophobic atoms do. The more accessible the atoms are, the more pronounced is the effect. E_{int} decreases when two hydrophobic or two hydrophilic atoms come close together in the hydrophilic and hydrophobic phases, respectively.

Integral membrane proteins and water-soluble proteins tend to form compact structures. For water-soluble proteins this is explained, since the protein does minimize its hydrophobic surface in contact with water. For integral membrane proteins, Rees and colleagues (1994) suggested a similar effect, as during membrane protein insertion interactions between adjacent lipids are disrupted and replaced by weaker protein-lipid interactions. E_{lip} accounts for the perturbation of the lipid bilayer due to peptide insertion. It is a defined as

$$E_{lip} = a_{lip} \sum_{i=1}^{N} S_{(i)} C_{(zi)} \quad (4)$$

where a_{lip} is an empirical factor fixed to −0.018. The concept of this equation is very simple, as E_{lip} increases with the surface of the protein in contact with lipids. The assumption is that lipids act as a pool of free-solvating CH_2 groups, although these groups are covalently linked in acyl chains. In order to perform the calculations the CH_2 groups have been assumed to have the same radius as water molecules, thus the atomic accessible surface is the same for water as for CH_2.

In previous calculations these two restraints have been tested by application to peptides (Ducarme et al., 1998), the configurations of which had been experimentally determined. The structures of the peptides have been fixed in α-helical conformations and no change of internal structure was allowed. This drastically simplified the problem as follows: first, only 3 degrees of freedom were considered (two rotations and one translation) so that the Monte Carlo procedure used is efficient. Second, Coulomb, van der Waals, hydrogen bonds, and torsion energies have been used as constants, thus the only three variable parameters of the simulation are z_0, α, and a_{lip}.

The peptide structures were constructed using Hyperchem 5.0 from Autodesk Inc., Sausalito, CA. The molecules are fully described (H included, no heavy atom) as this has an obvious effect on the accessible surface used in the calculations. The starting positions of peptides are determined by an algorithm that predicts the hydrophobic/hydrophilic interface of amphipathic peptides (Brasseur, 1991). The molecule is translated so that this interface is at z = 13.5 Å. A standard Monte Carlo procedure is then applied at 310 K for 10^5 steps (i.e., tries of moves) by

randomly translating (max. 1 Å) and rotating (max. 5°) the molecule. Each Monte Carlo calculation was run twice.

Calculations were performed on parallel hardware of 21 Tracor Europa Pentium Pro PC cadenced at 180 MHz connected by a 100-Mbyte Network and controlled by a HP Vectra VA Pentium Pro cadenced at 200 MHz. The calculation software (IMPALA) has been developed in our laboratory (Ducarme et al., 1998).

RESULTS

The peptides used in this study have been designed using alanine, leucine, and lysine residues, all known to have high or at least some propensity for α-helix formation (Cantor and Schimmel, 1980). This is particularly true in hydrophobic environments where conformations with extensive networks of hydrogen bonds are favored (Engelman et al., 1986; Bechinger, 1996). Line-fitting analysis of the CD-spectra shown in Fig. 1 indicate that all peptides exhibit a high degree of α-helical conformations in the presence of micelles or POPC small unilamellar vesicles and, therefore, confirm the secondary structure preferences of the amino acids used during the design of these peptides. Similar results are obtained when closely related peptides were investigated in non-oriented or oriented phospholipid membranes by FTIR spectroscopy (Zhang et al., 1995; Bechinger et al., 1999b). Helical wheel representations of the central 18 residues of the peptides investigated in this study are shown in Fig. 2.

Solid-state NMR spectroscopy of polypeptides that have been reconstituted into oriented phospholipid bilayers has previously been shown to provide a valuable tool for the analysis of the structure, dynamics, and orientational distribution of α-helical peptides in phospholipid bilayers (Smith et al., 1994; North et al., 1995; Bechinger, 1996). When compared to the ^{15}N chemical shift anisotropy, the ^{15}N chemical shift tensor of the amide bond exhibits only a small dependence on the chemical nature of the amino acid side chains and the secondary structure of the peptide (Shoji et al., 1989). The measurement of the ^{15}N chemical shift of isotopically labeled backbone amides, therefore, allows one to analyze approximate helix tilt angles in a straightforward manner. Whereas chemical shifts below the isotropic value ($\leq$100 ppm) are indicative of in-plane alignments, values around 210 ppm are characteristic for transmembrane helical peptides (Bechinger et al., 1999a). The anisotropic character of nuclear spin interactions has also been used in the past to experimentally determine the structure of bilayer-associated polypeptides. With at least two solid-state NMR parameters being measured for each peptide bond, the secondary structures of gramicidin or magainin 2 antibiotic peptides have been determined in phospholipid bilayers (Bechinger et al., 1993; Ketchem et al., 1993).

The peptides, designed and synthesized for this study, were incorporated into phospholipid membranes, which are mechanically oriented along glass surfaces with their normal parallel to the magnetic field direction. Proton-decoupled ^{31}P-NMR spectra of some of these preparations are shown in Fig. 3. In all samples used for further analysis one predominant ^{31}P resonance is observed at 30 ppm, demonstrating that the phospholipid molecules are well-oriented with their long axes parallel to the magnetic field direction. Smaller contributions to the total ^{31}P signal intensity are present at chemical shift frequencies between 30 and -15 ppm, indicating some misalignment of the membranes or conformational changes in the headgroup region due to the presence of peptides (Scherer and Seelig, 1989). The ob-

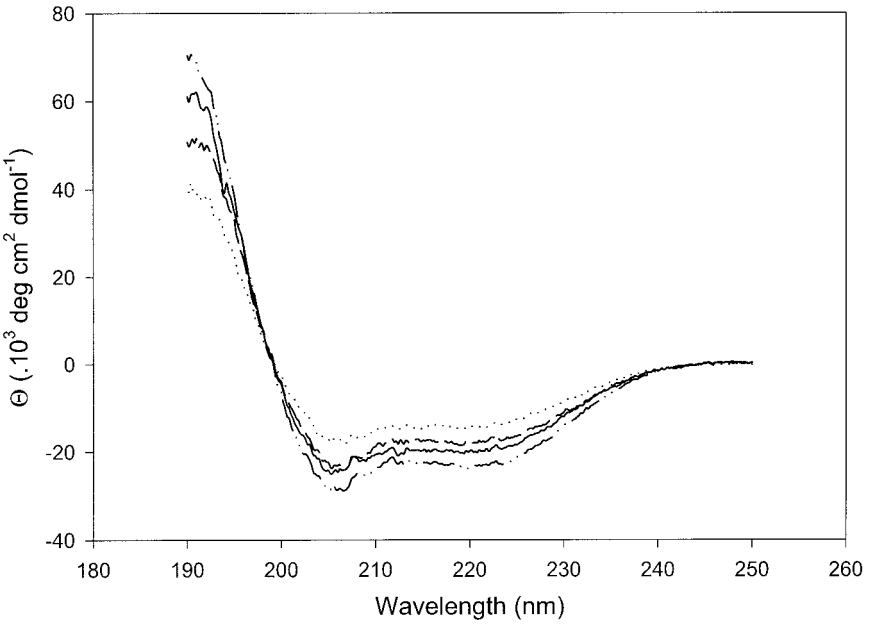

FIGURE 1 CD-spectroscopic analysis of 0.1 mM lysine-containing peptides in the presence of 30 mM sodium dodecyl sulfate, 20 mM Tris, pH 7.2. The spectral line shapes indicate a high propensity of all the peptides for helical secondary structures in membrane environments. The spectra shown are from LAK_1 (*solid line*), $LK_2^{<160}$ (*dotted line*), $LK_2^{<260}$ (*interrupted line*), and LAK_3 (*hatched line*).

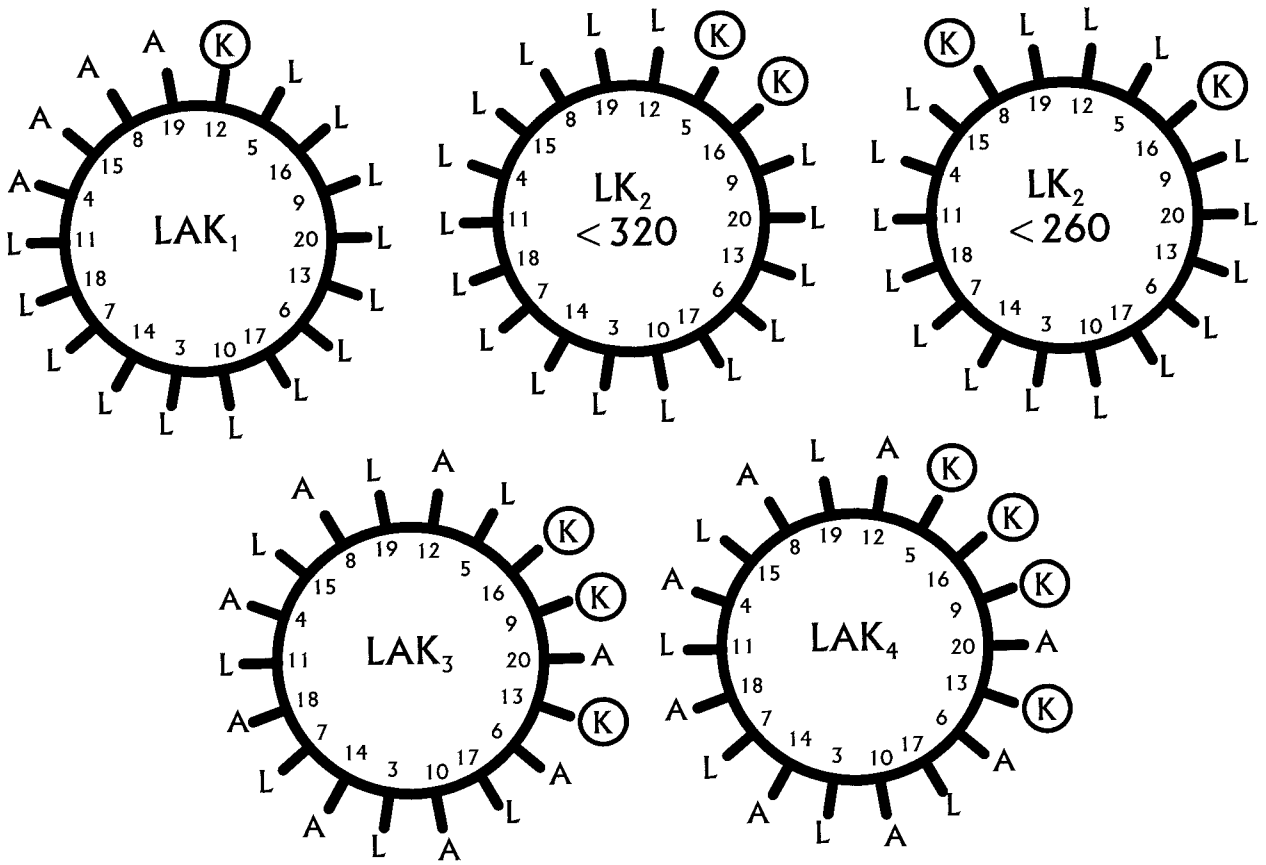

FIGURE 2 Edmundson helical wheel representations of residues 3–20 of the lysine-containing peptides. The labels inside the wheel indicate the names of the peptides and the positions in the sequence, respectively. The lysine residues are circled.

served ^{31}P chemical shift anisotropy of 45 ppm is characteristic for liquid crystalline phosphatidylcholine bilayers (Seelig, 1978). The proton-decoupled ^{15}N solid-state NMR spectra are therefore indicative of the orientational distribution of helical polypeptides with respect to the lipid bilayer (Bechinger, 1996; Lambotte et al., 1998; Bechinger et al., 1999a). In addition, the observation of chemical shift values close to the extremes of the chemical shift anisotropy (ranging from ~230 to ~60 ppm (Hartzell et al., 1987; Shoji et al., 1989; Lazo et al., 1995)) demonstrates that all of the peptides and labeled residues investigated are immobilized by strong interactions with lipid membranes (Fig. 4).

Whereas the more hydrophobic peptides LAK_1 and $LK_2^{<320}$ exhibit ^{15}N chemical shifts characteristic of transmembrane alignments (224 and 206 ppm, respectively, ±5 ppm), the more polar sequences LAK_3 and LAK_4 resonate at 59 and 80 ppm, respectively, typical for in-plane helical polypeptides (Figs. 4 and 7). LAK_1 exhibits transmembrane orientations also at 8 mol % concentrations. When this sample is tilted by 90° a single narrow resonance with a ^{15}N chemical shift of 78 ppm is observed (Bechinger, 2000). This result indicates that even at high peptide concentrations rotational averaging around the bilayer normal occurs.

$LK_2^{<260}$ shows a distribution of ^{15}N chemical shift resonances, which covers the whole width of the chemical shift anisotropy of the amide bond (~170 ppm). In order to test whether the amount of peptide added to the lipid membranes exceeds its "membrane solubility," spectra at reduced $LK_2^{<260}$-to-POPC molar ratio were also recorded. However, samples, which contain only 1 or 0.5 mol % peptide, exhibit an equally broad chemical shift distribution (not shown). The wide distribution of peptide alignments indicates that $LK_2^{<260}$, when associated with phospholipid membranes, exchanges slowly between different orientations on the 10^{-4} s time scale of the ^{15}N chemical shift anisotropy.

For molecular modeling calculations using the IMPALA algorithm (Ducarme et al., 1998) LAK_1, $LK_2^{<260}$, $LK_2^{<320}$, LAK_3, and LAK_4 have been assembled in an α-helical conformation, taking into account classical Φ and Ψ angles. The N and C termini are not protected and all atoms, including H, are explicit. Three different simulations were performed, one rigid body, one non-rigid body, and one rigid body at high temperature.

During the rigid body simulations 10^5 steps at 310 K were computed with a maximal move in each step equal to 1 Å of translation and 5° rotation around the mass center.

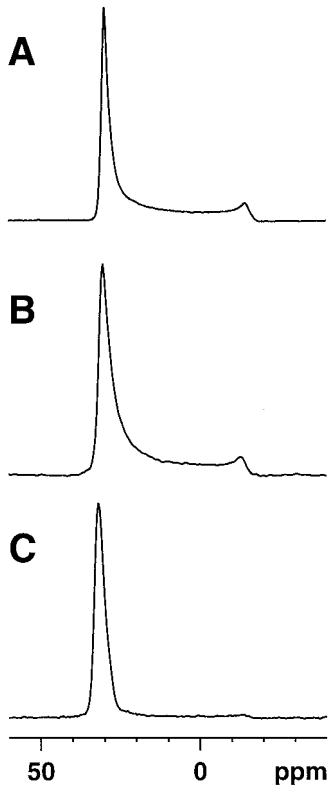

FIGURE 3 Proton-decoupled ^{31}P solid-state NMR spectra of POPC headgroups in samples also shown in Fig. 4. In the presence of (*A*) LAK_1, (*B*) $LK_2^{<260}$, (*C*) LAK_4.

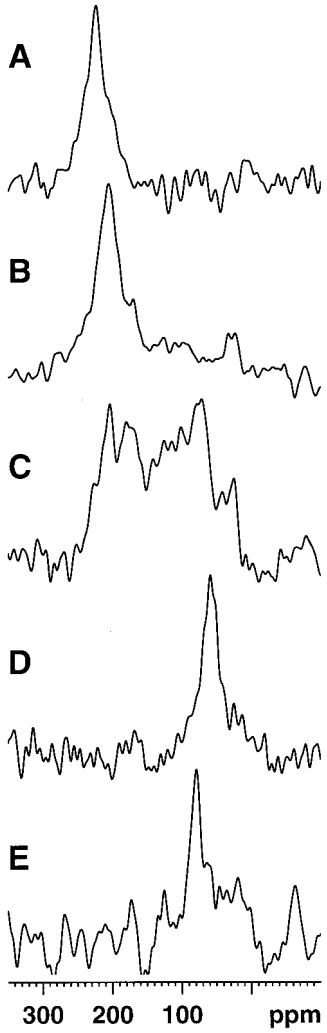

FIGURE 4 Proton-decoupled ^{15}N solid-state NMR spectra of lysine-containing peptides in oriented phosphatidylcholine (POPC) bilayers at neutral pH. The peptide-to-lipid molar ratios were 1:50. (*A*) LAK_1, (*B*) $LK_2^{<320}$, (*C*) $LK_2^{<260}$, (*D*) LAK_3, (*E*) LAK_4.

Fig. 5 *A* shows the absolute value of the angle of the α-helix axis as compared to the bilayer normal (90° is parallel to the interface, 0° or 180° are transmembrane). Fig. 5 *B* exhibits the penetration of the mass center. Clearly, LAK_1 and $LK_2^{<320}$ tend to adopt stable transmembrane orientations. The minimum of constraint corresponds to a tilt angle of the α-helices between 10° and 30° (Fig. 5 *A*) and the peptides equilibrate their mass centers close to the bilayer center (Fig. 5 *B*). The $LK_2^{<260}$ peptide is tilted at $\sim$20° with respect to the membrane interface, but its orientation seems less stable when compared to $LK_2^{<320}$ (not shown). The LAK_4 peptide is adsorbed to the interface (Fig. 5 *B*) with a helix tilt angle between 70° and 90° (Fig. 5 *A*). LAK_3 also equilibrates at the interface, but there are three minima at 60°, 70°, and 90°. The constraint between these minima has been overcome only once during the simulation. One of the low constraint configurations corresponds to an adsorbed orientation with an α-helical tilt angle around 70°, the lowest constraint configuration corresponds to an in-plane orientation (tilt angles around 90°).

During nonrigid body simulations 10^5 steps are computed at 310 K with a maximal movement during each step equal to 1 Å of translation and 5° of rotation. Structural changes of lateral side chain torsion angles with a 5° step size are allowed. The energy of interaction between nonbonded atoms is computed as the sum of the van der Waals, torsion, and electrostatic energies. These components are scaled by a factor of 100 in order to make the Monte Carlo simulation efficient. The general features of this simulation are identical to the rigid body simulation. Side-chain optimization does not modify the overall peptide behavior. The lysine side chains are adapting to the interface environment. In the case of LAK_4, the extremities of the lysine residues are strikingly well-gathered in the hydrophilic water environment. For LAK_3, some lysine residues at the center of the peptide are fully accessible to water in the adsorbed state, whereas they are hidden in 60° orientations. As a result, the hydrophilic patches of the hydrophobicity potential have almost disappeared (not shown).

High-temperature simulations are used to further investigate the constraint landscape. By raising the temperature the number of high-energy configurations screened by the

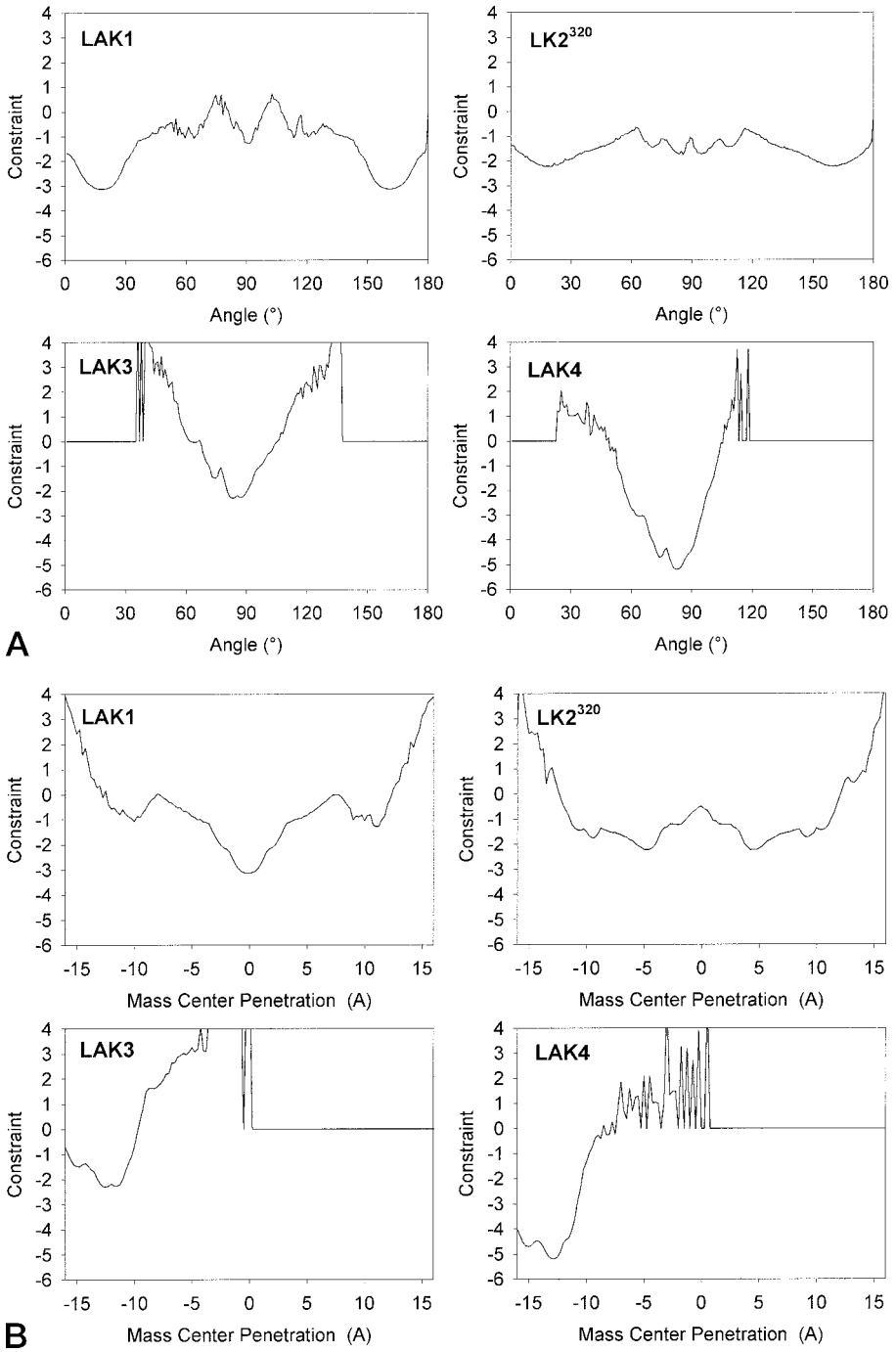

FIGURE 5 Contours of the Monte Carlo simulation of the LK peptides at low temperature (see text). (*A*) Sum of the restraints versus the angle between the helix axis and the membrane normal for various peptides (angle = 90° corresponds to an orientation parallel to the membrane surface). (*B*) Sum of the restraints versus the penetration of the mass center of the various peptides. ($z = 0$ is the bilayer center). The continuous line at zero constraint corresponds to non-explored domains of the plot in the simulation range (10^5 steps).

Monte Carlo procedure is increased. In these analyses we assessed that no other minima than those obtained during the first simulations exist. All parameters are identical to the rigid body simulation except the temperature, which is increased to 930 K (three times the usual temperature of 310 K). The constraints are plotted as a function of the α-helical tilt angle (Fig. 6 *A*) and the mass center penetration for the LK peptides (Fig. 6 *B*), respectively. Simulations at high temperature underline different minima of constraint corresponding to a transmembrane orientation for LAK_1 and $LK_2{}^{<320}$, as well as two symmetrical minima for LAK_4 corresponding to a parallel orientation at the interface.

A summary of the optimal location of the peptides with respect to the bilayer surface and their resulting hydrophobicity potentials are shown in Fig. 7, *A* and *B*, respectively.

DISCUSSION

A quantitative analysis of the NMR data is performed under the assumption that peptides with orientations parallel to the

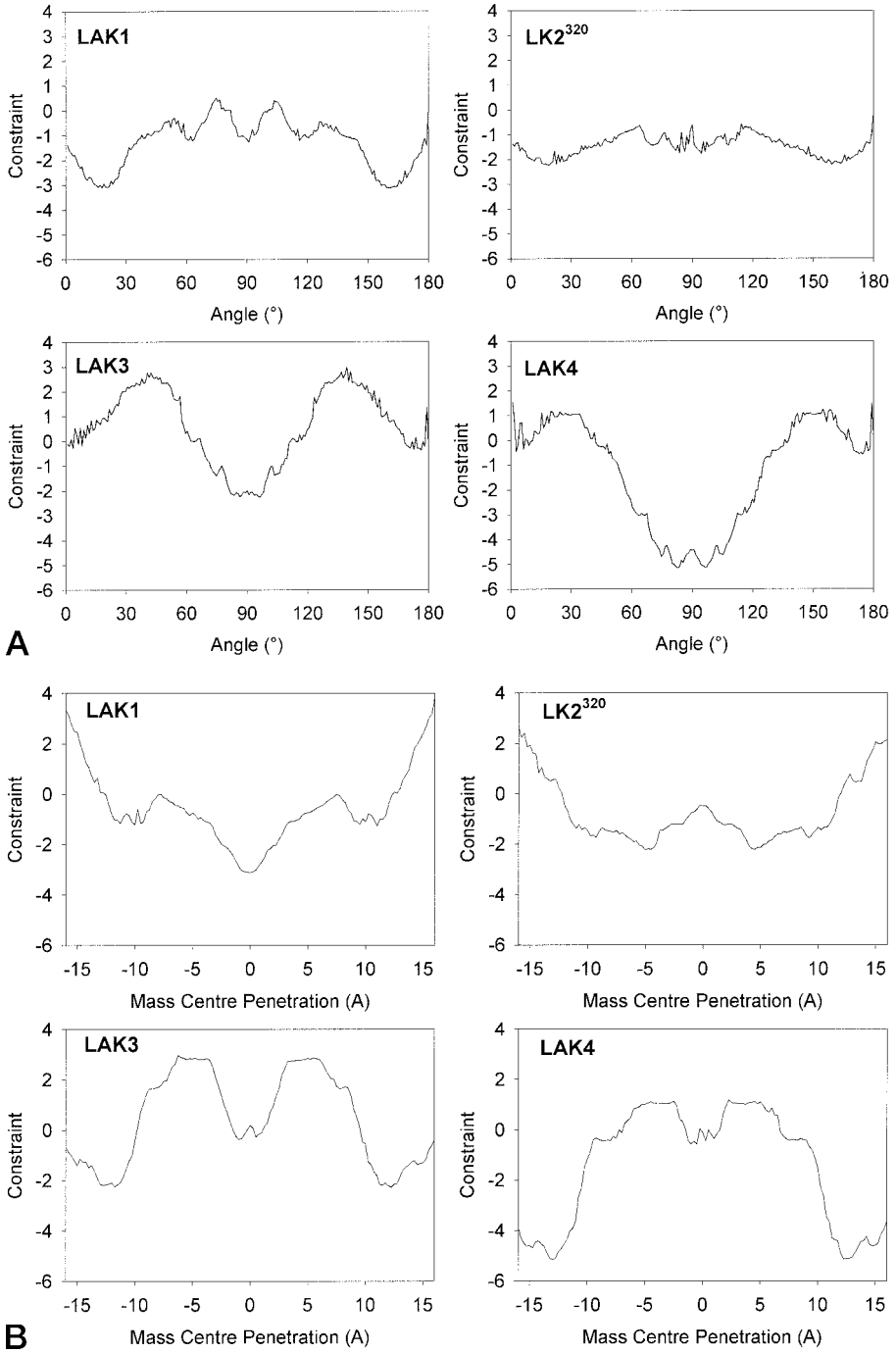

FIGURE 6 Contours of the Monte Carlo simulation of the LK peptides at high temperature (see text). (*A*) Sum of the restraints versus the angle of the helix axis and the membrane surface plane for the various peptides (angle = 90° corresponds to an in-plane orientation). (*B*) Sum of the restraints versus the penetration of the mass center of the various peptides. ($z = 0$ is the bilayer center)

membrane surface are in equilibrium with transmembrane alignments. The equilibrium constant is calculated according to $K = [TM]/[IP]$, where [TM] and [IP] are the surface concentrations of peptide in transmembrane and in-plane alignments, respectively. The Gibbs free energy that governs such a process is $\Delta G = \Delta G^{h} + \Delta G^{d} + \Delta G^{p} + \Delta G^{\#}$, with ΔG^{h} being the change in hydrophobic interactions during the transfer process, ΔG^{d} the energy required to discharge an amino acid side chain at a given pH, and ΔG^{p} the contribution of placing a polar or a discharged side chain in the hydrophobic membrane interior (Engelman et al., 1986; Bechinger, 1996). The term $\Delta G^{\#}$ includes changes in all other interactions such as hydrophobic mismatch energies, the lipophobic effect (Jähnig, 1983), or van der Waals interactions that occur during the process in-plane → transmembrane.

When compared to the energies of discharging an amino acid at neutral pH and consecutively placing a polar but uncharged residue in the membrane interior, the energy to place a charged amino acid side chain in the bilayer interior

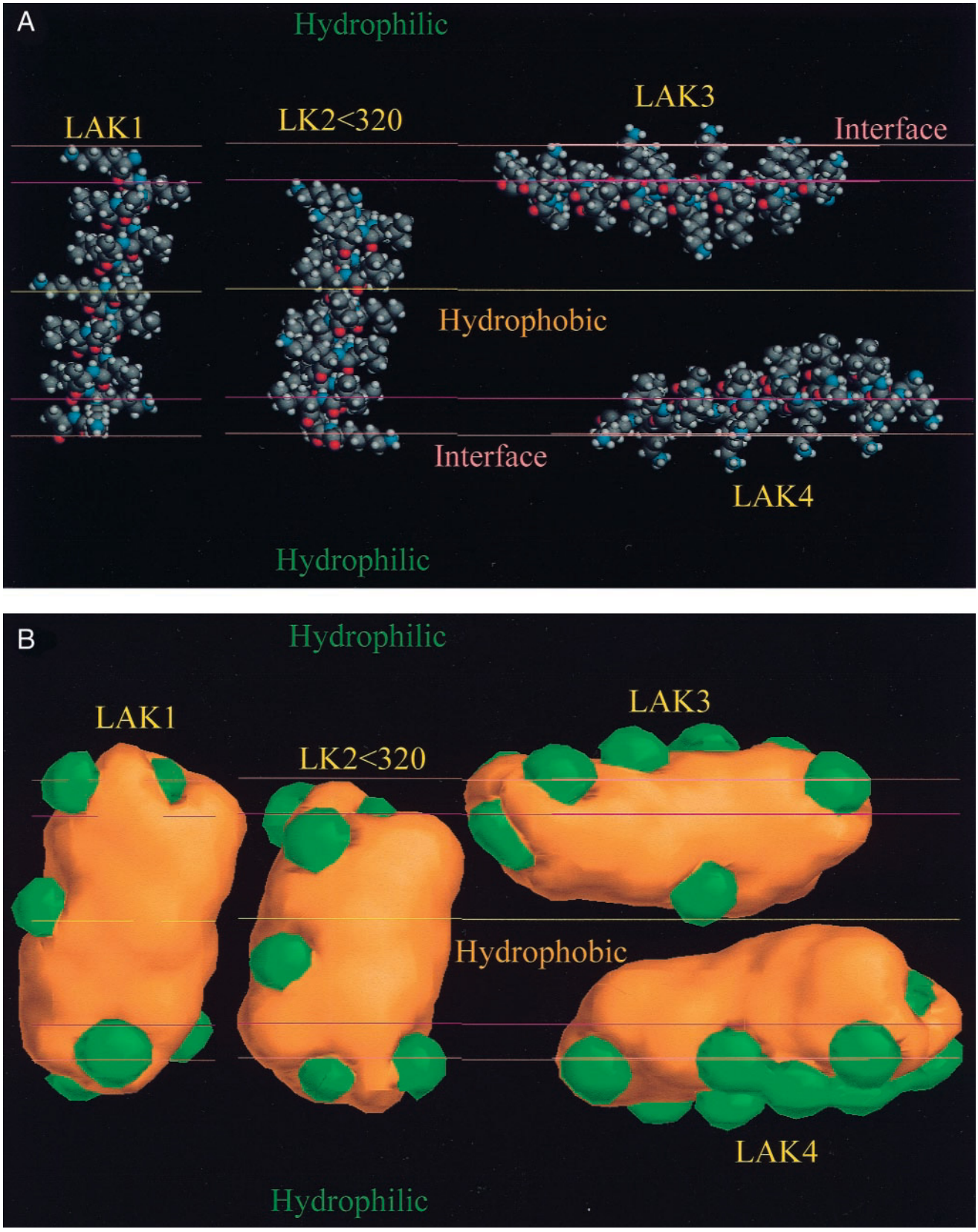

FIGURE 7 Graphical summary of the helical orientations of lysine-containing model peptides in oriented lipid bilayers observed by molecular modeling and proton-decoupled ^{15}N solid-state NMR spectroscopy. (*A*) The helices of LAK_1, $LK_2^{<320}$, LAK_3, and LAK_4 are represented as CPK models in their

is considerably more unfavorable. This former process at pH 7, therefore, forms the basis of some hydrophobicity tables (Engelman et al., 1986). From the chemical potentials of the Lewis acid or base of amino acid side chains it is, however, possible to calculate the energy to discharge a base at any given pH according to $\Delta G^{d} = n_i \cdot RT \cdot \ln r + 2.3RT\Sigma i\ (pK_i - pH)$, where i represents the amino acids that are discharged, n_i their total number, and $RT \ln r$ amounts to ~11.5 kJ/mol (Bechinger, 1996, 1997). The energy to discharge the lysine side chain at neutral pH amounts to ~32 kJ/mol ($pK - pH = 3.5$). Together with the hydrophobic contributions of four methylene segments ($\Delta G^{h} = -16$ kJ/mol) and the polar energy needed to move an NH_2-group into the hydrophobic interior of the membrane ($\Delta G^{p} \approx 20$ kJ/mol), the energetic costs of transferring a lysine side chain sums up to ~37 kJ/mol (Engelman et al., 1986). The transfer energies for lysine published by these and other authors range from 12 to 37 kJ/mol (von Heijne, 1981; Kyte and Doolittle, 1982; Engelman et al., 1986; White and Wimley, 1999). When compared to the Born energy of placing a charge in a hydrophobic environment, these values are reduced severalfold (Israelachvilli et al., 1980). Whereas the published transfer energies of hydrophilic amino acids in many cases exhibit a wide range of magnitudes, better agreement exists for those of hydrophobic residues, such as alanine and leucine.

More recently, transfer energies between the water phase and the bilayer interface have been measured (White and Wimley, 1999). These are only about half the size of the transfer energies between water and hydrophobic solvents. Within the interface the polarity changes rapidly and the potential energy of a particular amino acid is, therefore, dependent on factors such as peptide penetration depth and the amount of peptide-associated water. Nevertheless, by calculating the difference between the transfer energies water → interface minus water → membrane interior, an improved description of the in-plane-to-transmembrane helical transitions should be obtained (Table 1).

One could have imagined that LAK_1 penetrates into the bilayer in an in-plane orientation with the lysine side chain snorkeling to the surface (Segrest et al., 1990). At the same time the lipids arrange around the peptide to cover all the hydrophobic amino acids also when the peptide is oriented parallel to the membrane surface. The spectrum shown in Fig. 4 *A* indicates, however, that this peptide assumes transmembrane orientations that should place the lysine 12 residue in the hydrophobic core of the membrane. Geometrical considerations indicate that the length of the hydrophobic portion of the lipid (~15 Å) is too short to completely wrap around half the circumference of the peptide (18 Å when ignoring the lateral extension of the lipid). In addition, such a restrained conformation of the lipid would be energetically unfavorable. In particular, at the central core of the bilayer the order parameters are lowest and immobilization of these lipid segments seems entropically disfavored (Seelig, 1977). We therefore suggest that an in-plane orientation would result in the exposure to the aqueous environment of a ridge of hydrophobic amino acids. As a consequence, during an in-plane → transmembrane transition hydrophobic energy gains by several leucines, and alanines fully or partially compensate for the high transfer energy of one lysine. In addition, peptide reorientation results in modifications of other interactions ($\Delta G^{\#}$) such as hydrophobic mismatch energies, lipophobic effect, and van der Waals energies.

TABLE 1 The following contributions to the Gibbs free energy (kJ/mol) for the peptide reorientation from in-plane (IP) to transmembrane (TM) can explain the experimental data shown in Fig. 4. The transfer energies water → interface and water → octanol were used to estimate the transfer energies interface → membrane interior (White and Wimley, 1999, see text for details):

Peptide	ΔG_K	$\Delta G_A + \Delta G_L$*	$\Delta G\#$	ΔG	Alignment
LAK_1	7.6	−6.6	≤−7	≤−6	TM
$LK_2^{<320}$	7.6	−14.5		≤−6	TM
$LK_2^{<260}$	15.2	−11.6	−4	0	IP ⇔ TM
LAK_3	22.8	−1.5		≥+6	IP
LAK_4	30.4	+1.4		≥+6	IP

*At least six amino acids were assumed to be exposed to the water phase in the in-plane orientation (see text for details).

$LK_2^{<260}$ exhibits a close to equiintensive distribution of transmembrane and in-plane resonances and, therefore, ΔG is close to zero (Fig. 4 *C*). During an in-plane → transmembrane helix transition the high energies to transfer two lysine side chains into the membrane interior have to be compensated by hydrophobic energy contributions from several leucines as well as other contributions from, for example, lipid-lipid interactions ($\Delta G^{\#}$).

The second LK_2 peptide ($LK_2^{<320}$) exhibits a transmembrane orientation similar to LAK_1 (Fig. 4 *B*). The difference between $LK_2^{<320}$ and $LK_2^{<260}$ is probably a result of a close to interfacial location of lysine 5 ($LK_2^{<320}$), which allows for snorkeling of this side chain to the water phase in a direction parallel to the transmembrane helix (Monne et al., 1998). At the same time the many leucines of this peptide provide a sufficiently hydrophobic surface to pull the central lysine 13 into the bilayer interior (cf. above

optimal location relative to the membrane. The atoms are color-coded: *gray* for carbon, *white* for hydrogen, *red* for oxygen, and *blue* for nitrogen. (*B*) The molecular hydrophobicity potentials (Brasseur, 1991) of the peptides in the same orientations as shown in (*A*). Hydrophilic isopotential areas are shown in *green*, and hydrophobic isopotential areas in *orange*. Hydrophilic protuberances in the middle of the hydrophobic areas correspond to the extremities of the lysine side chains.

considerations for LAK_1). Finally, the unfavorable interactions of placing three or four lysines in the membrane interior result in stable in-plane orientations of the LAK_3 and LAK_4 peptides (Fig. 4, *D* and *E*).

The molecular modeling calculations are in good agreement with the NMR measurements. Indeed, in both spectroscopic and modeling experiments LAK_1 and $LK_2^{<320}$ are oriented in transmembrane configurations, and LAK_3 as well as LAK_4 assume stable orientations parallel to the interface. NMR measurements show a wide distribution of orientations for $LK_2^{<260}$, in agreement with molecular modeling calculations, which indicate that the peptide can adopt many different alignments and mean center penetrations.

The molecular modeling and NMR data agree surprisingly well when considering the simplified model of a lipid bilayer that has been used during the calculations. A more detailed description of the molecular interactions within the lipid membranes would require a more explicit description of the shape of the lipids and peptides involved. For example, whereas transmembrane α-helical polypeptides of ~20 amino acids match the thickness of the hydrophobic core region of the bilayer (~30 Å) well, the radius of an in-plane intercalated helix (5–6 Å) is insufficient to fill the thickness of one lipid monolayer completely. This is particularly true for peptides with a small hydrophobic angle, such as magainins ($<160^o$), where a distance of 10 Å has been measured from the hydrophobic face of the peptide to the bilayer center (Matsuzaki et al., 1994). The in-plane intercalation of a peptide, therefore, increases the surface area of the bilayer without changing the volume of the membrane to the same extent. The space underneath the intercalated peptide helix is filled in by neighboring and opposing lipid acyl chains, and as a consequence results in the reduction of the average membrane thickness (Ludtke et al., 1995). These considerations suggest that the "hydrophobic mismatch" of an in-plane intercalated peptide introduces energy contributions favoring the in-plane-to-transmembrane transition. Hydrophobic mismatch energies have been theoretically described in previous publications, but to our knowledge so far not been determined experimentally (Mouritsen and Bloom, 1984). They do, however, contribute to $\Delta G^{\#}$, estimates of which can be obtained from semiquantitative analyses of experimental solid-state NMR data (Tables 1 and 2).

The two-state equilibrium describing the topology of lysine-containing hydrophobic peptides has so far ignored the possibility of oligomer formation within the membrane. From our solid-state NMR measurements on 90^o tilted samples we can exclude the formation of large extended aggregates, in agreement with previous investigations on related peptides such as magainin 2, Ac-$K_2L_{24}K_2$-amide, $GW_2(LA)_8LW_2A$, and $GK_2(LA)_8LK_2A$ (Schümann et al., 1997; Subczynski et al., 1998; de Planque et al., 1999), or on bacteriorhodopsin when reconstituted into model membranes (Lewis and Engelman, 1983). Although electrostatic repulsion, exposure of hydrophobic residues to water-filled pores, and entropic contributions disfavor the formation of transmembrane helical bundles, our NMR results alone do not exclude formation of oligomers consisting of few lysine-containing peptides. The modeling calculations presented in this paper, therefore, provide important additional insight that helps to understand the interaction contributions during the transition of monomeric helices from in-plane to transmembrane alignments. The possibility of additional equilibria that involve association interactions of membrane-associated peptides is currently being tested experimentally in our laboratory.

TABLE 2 The following contributions to the Gibbs free energy (kJ/mol) for the peptide reorientation from in-plane (IP) to transmembrane (TM) can explain the experimental data shown in Fig. 4 (using the values by Engelman et al. 1986, see text for details):

Peptide	$\Delta G^d + \Delta G^P$	ΔG^h*	$\Delta G\#$	ΔG	Alignment
LAK_1	52	−59	≤0	≤−6	TM
$LK_2^{<320}$	52	−94	≤0	≤−42	TM
$LK_2^{<260}$	104	−78	−26	0	IP ⇔ TM
LAK_3	156	−72	−26	+58	IP
LAK_4	208	−75	−26	+107	IP

*At least six amino acids were assumed to be exposed to the water phase in the in-plane orientation.

We are grateful to Ingrid Neidhart for the synthesis of some of the peptides. The members of Luis Moroder's group have helped during the synthesis of the more difficult sequences and allowed access to their CD spectrophotometer. We gratefully acknowledge the support of Dieter Oesterhelt, who provided access to the Millipore peptide synthesizer of his department. R.B. is Research Director at the National Funds for Scientific Research in Belgium (FNRS).

This work was supported by the Interuniversity Poles of Attraction Programme–Belgian State, Prime Minister's Office–Federal Office for Scientific, Technical and Cultural Affairs' PAI contact no. P4/03.

REFERENCES

Bechinger, B. 1996. Towards membrane protein design: pH dependent topology of histidine-containing polypeptides. *J. Mol. Biol.* 263: 768–775.

Bechinger, B. 1997. Structure and functions of channel-forming polypeptides: magainins, cecropins, melittin and alamethicin. *J. Membr. Biol.* 156:197–211.

Bechinger, B. 1999. The structure, dynamics and orientation of antimicrobial peptides in membranes by solid-state NMR spectroscopy. *Biochim. Biophys. Acta.* 1462:157–183.

Bechinger, B. 2000. Biophysical investigations of membrane perturbations by polypeptides using solid-state NMR spectroscopy. *Mol. Membr. Biol.* in press.

Bechinger, B., R. Kinder, M. Helmle, T. B. Vogt, U. Harzer, and S. Schinzel. 1999a. Peptide structural analysis by solid-state NMR spectroscopy. *Biopolymers.* 51:174–190.

Bechinger, B., and S. J. Opella. 1991. Flat-coil probe for NMR spectroscopy of oriented membrane samples. *J. Magn. Reson.* 95:585–588.

Bechinger, B., J. M. Ruysschaert, and E. Goormaghtigh. 1999b. Membrane helix orientation from linear dichroism of infrared attenuated total reflection spectra. *Biophys. J.* 76:552–563.

Bechinger, B., M. Zasloff, and S. J. Opella. 1993. Structure and orientation of the antibiotic peptide magainin in membranes by solid-state NMR spectroscopy. *Protein Sci.* 2:2077–2084.

Belrhali, H., P. Nollert, A. Royant, C. Menzel, J. P. Rosenbusch, E. M. Landau, and E. Pebay-Peyroula. 1999. Protein, lipid and water organization in bacteriorhodopsin crystals: A molecular view of the purple membrane at 1.9 Angstrom resolution. *Structure*. 7:909–917.

Ben-Shaul, A., N. Ben-Tal, and B. Honig. 1996. Statistical thermodynamic analysis of peptide and protein insertion into lipid membranes. *Biophys. J.* 71:130–137.

Ben-Tal, N., A. Ben-Shaul, A. Nicholls, and B. Honig. 1996. Free-energy determinants of a-helix insertion into lipid bilayers. *Biophys. J.* 70: 1803–1812.

Bevins, C. L., and M. Zasloff. 1990. Peptides from Frog Skin. *Annu. Rev. Biochem.* 59:395–441.

Boman, H. G. 1995. Peptide antibiotics and their role in innate immunity. *Annu. Rev. Immunol.* 13:61–92.

Brasseur, R. 1991. Differentiation of lipid-associating helices by use of three-dimensional molecular hydrophobicity potential calculations. *J. Biol. Chem.* 266:16120–16127.

Cantor, C. R., and P. R. Schimmel. 1980. Biophysical Chemistry, Part 1. W. H. Freeman and Co., New York.

Chen, G. C., and J. T. Yang. 1977. Two point calibration of circular dichrometer with d-10-camphorsulfonic acid. *Anal. Lett.* 10:1195–1207.

Cruciani, R. A., J. L. Barker, G. Raghunathan, H. R. Guy, M. Zasloff, and E. F. Stanley. 1992. Magainin 2, a natural antibiotic from frog skin, forms ion channels in lipid bilayer membranes. *Eur. J. Pharmacol.* 226:287–296.

Cruciani, R. A., J. L. Barker, M. Zasloff, H. Chen, and O. Colamonici. 1991. Antibiotic magainins exert cytolytic activity transformed cell lines through channel formation. *Proc. Natl. Acad. Sci. USA.* 88:3792–3796.

Deisenhofer, J., O. Epp, K. Miki, R. Huber, and H. Michel. 1985. Structure of the protein subunits in the photosynthetic reaction centre of *Rhodopseudomonas viridis* at 3 A resolution. *Nature.* 318:618.

Dempsey, C. E. 1990. The actions of melittin on membranes. *Biochim. Biophys. Acta.* 1031:143–161.

de Planque, M. R. R., J. A. W. Kruijtzer, R. M. J. Liskamp, D. Marsh, D. V. Greathouse, R. E. Koeppe, B. De Kruijff, and J. A. Killian. 1999. Different membrane anchoring positions of tryptophan and lysine in synthetic transmembrane alpha-helical peptides. *J. Biol. Chem.* 274: 20839–20846.

Doak, D. G., D. Mulvey, K. Kawaguchi, J. Villalain, and I. D. Campbell. 1996. Structural studies of synthetic peptides dissected from the voltage-gated sodium channel. *J. Mol. Biol.* 258:672–687.

Ducarme, P., M. Rahman, and R. Brasseur. 1998. IMPALA: a simple restraint field to simulate the biological membrane in molecular structure studies. *Proteins.* 30:357–371.

Duclohier, H., G. Molle, and G. Spach. 1989. Antimicrobial peptide magainin I from Xenopus skin forms anion-permeable channels in planar lipid bilayers. *Biophys. J.* 56:1017–1021.

Eisenhaber, F., and P. Argos. 1993. Improved strategy in analytic surface calculation for molecule systems: handling singularities and computational efficiency. *J. Comp. Chem.* 11:272–1280.

Engelman, D. M., T. A. Steitz, and A. Goldman. 1986. Identifying nonpolar transbilayer helices in amino acid sequences of membrane proteins. *Annu. Rev. Biophys. Biophys. Chem.* 15:321–353.

Gibson, B. W., L. Poulter, D. H. Williams, and J. E. Maggio. 1986. Novel peptide fragments originating from PGL and the caerulein and xenopsin precursors from *Xenopus laevis*. *J. Biol. Chem.* 261:5341–5349.

Haimovich, B., and J. C. Tanaka. 1995. Magainin-induced cytotoxicity in eukaryotic cells: kinetics, dose-response and channel characteristics. *Biochim. Biophys. Acta.* 1240:149–158.

Hartzell, C. J., M. Whitfield, T. G. Oas, and G. P. Drobny. 1987. Determination of the 15N and 13C chemical shift tensors of L-[13C]alanyl-L-[15N]alanine from the dipole-coupled powder patterns. *J. Am. Chem. Soc.* 109:5966–5969.

Hoffmann, W., K. Richter, and G. Kreil. 1983. A novel peptide designated PYL and its precursor as predicted from cloned mRNA of *Xenopus laevis* skin. *EMBO J.* 2:711–714.

Hultmark, D. 1994. Drosophila as a model system for antibacterial peptides. *Ciba Foundation Symposium.* 186:107–119.

Israelachvilli, J. N., S. Marcelja, and R. G. Horn. 1980. Physical principles of membrane organization. *Q. Rev. Biophys.* 13:121–200.

Jähnig, F. 1983. Thermodynamics and kinetics of protein incorporation into membranes. *P. N. A. S. USA.* 80:3691–3695.

Juretic, D., R. W. Hendler, F. Kamp, W. S. Caughey, M. Zasloff, and H. V. Westerhoff. 1994. Magainin oligomers reversibly dissipate the proton electrochemical gradient in cytochrome oxidase liposomes. *Biochemistry.* 33:4562–4570.

Ketchem, R. K., W. Hu, and T. A. Cross. 1993. High-resolution conformation of gramicidin A in a lipid bilayer by solid-state NMR. *Science.* 261:1457–1460.

Kyte, J., and R. F. Doolittle. 1982. A simple method for displaying the hydropathic character of a protein. *J. Mol. Biol.* 157:105–132.

Lambotte, S., P. Jasperse, and B. Bechinger. 1998. Orientational distribution of alpha-helices in the colicin B and E1 channel domains: a one- and two dimensional 15N solid-state NMR investigation in uniaxially aligned phospholipid bilayers. *Biochemistry.* 37:16–22.

La Rocca, P., Y. Shai, and M. S. P. Sansom. 1999. Peptide/bilayer interactions: simulations of dermaseption B, an antimicrobial peptide. *Biophys. Chem.* 76:145–159.

Lazo, N. D., W. Hu, and T. A. Cross. 1995. Low-temperature solid-state ^{15}N NMR characterization of polypeptide backbone librations. *J. Magn. Res.* 107:43–50.

Lewis, B. A., and D. M. Engelman. 1983. Bacteriorhodopsin remains dispersed in fluid phospholipid bilayers over a wide range of bilayer thicknesses. *J. Mol. Biol.* 166:203–210.

Ludtke, S. J., K. He, W. T. Heller, T. A. Harroun, L. Yang, and H. W. Huang. 1996. Membrane pores induced by magainin. *Biochemistry.* 35:13723–13728.

Ludtke, S., K. He, and H. Huang. 1995. Membrane thinning caused by magainin 2. *Biochemistry.* 34:16764–16769.

Matsuzaki, K., O. Murase, H. Tokuda, S. Funakoshi, N. Fujii, and K. Miyajima. 1994. Orientational and aggregational states of magainin 2 in phospholipid bilayers. *Biochemistry.* 33:3342–3349.

Milik, M., and J. Skolnick. 1993. Insertion of peptide chains into lipid membranes: an off-lattice Monte Carlo dynamics model. *Proteins.* 15: 10–25.

Monne, M., I. Nilsson, M. Johansson, N. Elmhed, and G. von Heijne. 1998. Positively and negatively charged residues have different effects on the position in the membrane of a model transmembrane helix. *J. Mol. Biol.* 284:1177–1183.

Mouritsen, O. G., and M. Bloom. 1984. Mattress model of lipid-protein interactions in membranes. *Biophys. J.* 46:141–153.

North, C. L., M. Barranger-Mathys, and D. S. Cafiso. 1995. Membrane orientation of the N-terminal segment of alamethicin determined by solid-state ^{15}N-NMR. *Biophys. J.* 69:2392–2397.

Ohsaki, Y., A. F. Gazdar, H. Chen, and B. E. Johnson. 1992. Antitumor activity of magainin analogues against human lung cancer cell lines. *Cancer Res.* 52:3534–3538.

Picot, D., P. J. Loll, and R. M. Garavito. 1994. The x-ray crystal structure of the membrane protein prostaglandin H2 synthase-1. *Nature.* 367: 243–249.

Pines, A., M. G. Gibby, and J. S. Waugh. 1973. Proton-enhanced NMR of dilute spins in solids. *J. Chem. Phys.* 59:569–590.

Rance, M., and R. A. Byrd. 1983. Obtaining high-fidelity spin-1/2 powder spectra in anisotropic media: phase-cycled Hahn echo spectroscopy. *J. Magn. Reson.* 52:221–240.

Rees, D. C., A. J. Chirino, K.-H. Kim, and H. Komiya. 1994. Membrane protein structure and stability: implications of the first crystallographic analysis. *In* Membrane Protein Structure: Experimental Approaches. S. H. White, editor. Oxford University Press, New York. 3–26.

Sansom, M. S. 1993. Alamethicin and related peptaibols—model ion channels. *Eur. Biophys. J.* 22:105–124.

Scherer, P. G., and J. Seelig. 1989. Electric charge effects on phospholipid headgroups. phosphatidylcholine in mixtures with cationic and anionic amphiles. *Biochemistry.* 28:7720–7727.

Schümann, M., M. Dathe, T. Wieprecht, M. Beyermann, and M. Bienert. 1997. The tendency of magainin to associate upon binding to phospholipid bilayers. *Biochemistry.* 36:4345–4351.

Seelig, J. 1977. Deuterium magnetic resonance: theory and application to lipid membranes. *Q. Rev. Biophys.* 10:353–418.

Seelig, J. 1978. ^{31}P-NMR and the headgroup structure of phospholipids in membranes. *Biochim. Biophys. Acta.* 515:105–140.

Segrest, J. P., H. De Loof, J. G. Dohlmann, C. G. Brouillette, and G. M. Anatharamaiah. 1990. Amphipathic helix motif: classes and properties. *Proteins: Struct., Funct., Genet.* 8:103–117.

Shoji, A., T. Ozaki, T. Fujito, K. Deguchi, S. Ando, and I. Ando. 1989. ^{15}N-NMR chemical shift tensors and conformation of some ^{15}N-labeled polypeptides in the solid state. *Macromolecules.* 22:2860–2863.

Smith, R., F. Separovic, T. J. Milne, A. Whittaker, F. M. Bennett, B. A. Cornell, and A. Makriyannis. 1994. Structure and orientation of the pore-forming peptide, melittin, in lipid bilayers. *J. Mol. Biol.* 241: 456–466.

Soballe, P. W., W. L. Maloy, M. L. Myrga, L. S. Jacob, and M. Herlyn. 1995. Experimental local therapy of human melanoma with lytic magainin peptides. *Int. J. Cancer.* 60:280–284.

Subczynski, W. K., R. N. Lewis, R. N. McElhaney, R. S. Hodges, J. S. Hyde, and A. Kusumi. 1998. Molecular organization and dynamics of 1-palmitoyl-2-oleoylphosphatidylcholine bilayers containing a transmembrane alpha-helical peptide. *Biochemistry.* 37:3156–3164.

Vaz Gomes, A., A. de Waal, J. A. Berden, and H. V. Westerhoff. 1993. Electric potentiation, cooperativity, and synergism of magainin peptides in protein-free liposomes. *Biochemistry.* 32:5365–5372.

Vogt, T. C. B., and B. Bechinger. 1999. The interactions of histidine-containing amphipathic helical peptide antibiotics with lipid bilayers: the effects of charges and pH. *J. Biol. Chem.* 274:29115–29121.

von Heijne, G. 1981. Membrane proteins: the amino acid composition of membrane penetrating segments. *Eur. J. Biochem.* 120:275–278.

White, S. H. 1994. Hydropathy plots and the prediction of membrane protein topology. *In* Membrane Protein Structure: Experimental Approaches. S. H. White, editor. Oxford University Press, New York. 97–124.

White, S. H., and W. C. Wimley. 1999. Membrane protein folding and stability: physical principles. *Annu. Rev. Biophys. Biomol. Struct.* 28: 319–365.

Zhang, Y. P., R. N. Lewis, G. D. Henry, B. D. Sykes, R. S. Hodges, and R. N. McElhaney. 1995. Peptide models of helical hydrophobic transmembrane segments of membrane proteins. 1. Studies of the conformation, intrabilayer orientation, and amide hydrogen exchangeability of Ac-K2-(LA)12-K2-amide. *Biochemistry.* 34:2348–2361.